11-2012

Trajectories of Rolling Marbles on Various Funnels

Lars Q. English
Dickinson College

A. Mareno

Trajectories of rolling marbles on various funnels

L. Q. English
Department of Physics and Astronomy, Dickinson College, Carlisle, Pennsylvania 17013

A. Mareno
Department of Mathematics and Computer Science, Penn State Harrisburg, Middletown, Pennsylvania 17013

(Received 28 March 2012; accepted 5 August 2012)

We investigate the trajectories of a small marble constrained to roll on frictionless surfaces, called funnels, of varying shapes. Actual coin funnels have a hyperbolic surface, and here we disprove the common claim that the orbits of the rolling marble or coin are the same as the Kepler orbits for planets revolving around the sun. In fact, it is straightforward to show that for no funnel surface can the Kepler orbits be recovered. Furthermore, we find that the types of trajectories that can arise depend heavily on the funnel shape.
[http://dx.doi.org/10.1119/1.4747481]

I. INTRODUCTION

Coin funnels have become quite commonplace in science museums and are increasingly appearing in malls and other public spaces. Typically, these funnels are hyperbolic surfaces featuring a chute to launch a coin or marble. The chute is often configured to produce a nearly circular orbit for the coin once it is released onto the funnel surface. The orbit's radius, however, gradually decays due to energy dissipation, and the coin is irretrievably sucked into the funnel. In this way, these funnels double as income generators. In fact, oftentimes the visitor is challenged to find out if the coin size affects the orbit—in a clever attempt to collect quarters in addition to pennies. Alternatively, one can also launch the coin or marble directly onto the surface (i.e., without using the chute). Then other types of orbits emerge, such as non-repeating loops resembling flower petals. In the planetary problem, bound orbits deviating from a circle must necessarily be ellipses. Therefore, even a cursory observation of motion in a funnel reveals that these two problems are different. This difference arises despite the identical functional forms of the potential energies involved. In fact, we show that for no surface is it possible to obtain Kepler orbits (except for circles).

We examine three different funnel surfaces: inverse-power surfaces whose height is proportional to radius to the power –1, –2, and –3. We determine the equations of motion for a rolling marble on each. The three surfaces were chosen partly for their apparent graphical similarity: Each surface resembles an infinitely deep well at its center and asymptotically approaches zero for large radii. Although superficially the surfaces have similar shapes, the types of orbits that arise can be categorically different. To see why this happens, we take a dynamical systems approach to determine the stability of circular orbits in each case and again find intriguing differences. Note that one straightforward way of constructing a surface with an exponent of 2/3 is by placing a ball on an elastic sheet.[1]

The development in this paper is aimed at the level of a junior/senior course in classical mechanics, and we believe that a number of elements herein could be woven into such a course rather seamlessly. In this context, the coin funnel offers an intriguing example from everyday life which illustrates the power of Lagrangian mechanics while also making contact with the qualitative theory of differential equations.

II. DERIVATION OF THE MAIN EQUATIONS

We examine the case of a very small marble rolling without slippage on a funnel surface. The reason we chose to restrict the discussion to small marbles is that as the marble radius approaches zero, so does its angular momentum and the torque acting upon it. In fact, the full problem of a ball rolling without slippage is somewhat more difficult as it involves non-holonomic constraints between generalized velocities involving rotational and translational motion.[2,3] Standard Lagrangian mechanics is not equipped to incorporate such constraints, and a more general set of equations (sometimes called the Poincare equations[4]) has to be invoked. However, it can be shown[3,4] that in the absence of external torques, a marble behaves as if its inertial mass had increased by a constant factor proportional to its moment of inertia—and the small radius guarantees negligible torques.

In the case of rolling on a level surface that is "perfectly rough,"[3] no frictional forces exist at the point of contact. Such reaction forces will arise on curved surfaces (for which the marble experiences a net external force), but these do not give rise to energy dissipation; instead they cause a change in angular momentum.[4] Therefore, friction does not enter explicitly.

Furthermore, we restrict the discussion to funnel surfaces that are cylindrically symmetric, so their shape can be described simply as height as a function of radius: $z = z(r)$. Since the object has to stay on the funnel surface, a relationship between two of the three cylindrical coordinates is introduced and this relationship represents a constraint on the dynamics. The ensuing motion is difficult to predict in the Newtonian framework, as the constraint immediately gives rise to complicated normal forces. The strength of the Lagrangian approach is that forces of constraint can be ignored when working with a reduced number of generalized coordinates; in this way, Lagrangian mechanics is ideally suited to incorporate such constraints between coordinates.

The shape of each of our funnels is determined by the function $z(r)$, so the potential energy of the marble is $mgz(r)$. The translational kinetic energy in cylindrical coordinates is

$$T = \frac{1}{2}m\mathbf{v}^2 = \frac{1}{2}m[\dot{r}^2 + r^2\dot{\phi}^2 + \dot{z}^2], \tag{1}$$

and the marble's spin contributes an additional $T = (1/2)I\omega^2 = (1/2)I\mathbf{v}^2/R^2 = (1/5)m\mathbf{v}^2$, where the

marble is considered a solid sphere. Note that even when the marble size goes to zero, this rotational contribution does not vanish. Hence, we can write the Lagrangian as

$$L = \frac{1}{2}\hat{m}[\dot{r}^2 + r^2\dot{\phi}^2 + \dot{z}^2] - mgz(r), \tag{2}$$

where $\hat{m} = (7/5)m$.

Next, we derive the associated Euler-Lagrange equations. A straightforward calculation shows that the ϕ equation reduces to

$$\hat{m}r^2\dot{\phi} = \text{constant} = \ell. \tag{3}$$

We remark that Eq. (3) implies angular momentum conservation, and this holds independent of the type of surface we investigate. To obtain the r equation, we first use the chain rule to deduce that

$$\dot{z} = \frac{dz}{dr}\dot{r}, \qquad \frac{d}{dt}\left(\frac{dz}{dr}\right) = \frac{d^2z}{dr^2}\dot{r}, \tag{4}$$

and so

$$\frac{\partial L}{\partial r} = \hat{m}r\dot{\phi}^2 + \hat{m}\frac{dz}{dr}\frac{d^2z}{dr^2}\dot{r}^2 - mg\frac{dz}{dr}, \tag{5}$$

$$\frac{\partial L}{\partial \dot{r}} = \hat{m}\dot{r} + \hat{m}\left(\frac{dz}{dr}\right)^2\dot{r}. \tag{6}$$

This leads to the remaining part of the Euler-Lagrange equation,

$$\frac{d}{dt}\left(\frac{\partial L}{\partial \dot{r}}\right) = \hat{m}\ddot{r} + \hat{m}\left(\frac{dz}{dr}\right)^2\ddot{r} + 2\hat{m}\frac{dz}{dr}\frac{d^2z}{dr^2}\dot{r}^2. \tag{7}$$

Note that by Eq. (3), $\dot{\phi}^2 = \ell^2/\hat{m}^2r^4$. Now, using Eqs. (5)–(7) and dividing by $\hat{m}$, we obtain the governing equation

$$\left[1 + \left(\frac{dz}{dr}\right)^2\right]\ddot{r} + \frac{dz}{dr}\frac{d^2z}{dr^2}\dot{r}^2 + \frac{5g}{7}\frac{dz}{dr} - \frac{\ell^2}{\hat{m}^2r^3} = 0. \tag{8}$$

The solution of this equation will yield $r(t)$. In principle, we can then also obtain $\phi(t)$ via integration of Eq. (3). The set $[r(t), \phi(t)]$ defines the trajectory of the marble on the funnel surface parametrically.

The form of this and subsequent equations can be simplified somewhat by introducing dimensionless space and time variables. To do so, we make the substitutions

$$\tilde{z} = az, \quad \tilde{r} = ar, \quad \tau = bt, \tag{9}$$

where

$$a = \frac{7}{5g}\left(\frac{\hat{m}(5g)^2}{49\ell}\right)^{2/3}, \qquad b = \left(\frac{\hat{m}(5g)^2}{49\ell}\right)^{1/3}. \tag{10}$$

With these dimensionless variables, Eq. (8) becomes

$$\left[1 + \left(\frac{d\tilde{z}}{d\tilde{r}}\right)^2\right]\frac{d^2\tilde{r}}{d\tau^2} + \frac{d\tilde{z}}{d\tilde{r}}\frac{d^2\tilde{z}}{d\tilde{r}^2}\left(\frac{d\tilde{r}}{d\tau}\right)^2 + \frac{d\tilde{z}}{d\tilde{r}} - \frac{1}{\tilde{r}^3} = 0. \tag{11}$$

III. A SURFACE PROPORTIONAL TO r^{-1}

First we let $z(r) = -k/r$, where k is assumed to be a positive constant. This is the shape realized by actual coin funnels, commonly referred to as hyperbolic funnels.[5] Then the potential energy of the marble is $U(r) = -mgk/r$. In this case, the potential energy of the marble has the same form as the gravitational potential energy between two masses, $U(r) = -Gm_1m_2/r$. It is this correspondence between the potential energies that gives rise to the claim that the marbles in this funnel mimic planetary motion.[5] This claim, however, is not entirely correct, as we now demonstrate.

For this choice of $z(r)$, Eq. (8) becomes

$$\left(1 + \frac{k^2}{r^4}\right)\ddot{r} - \frac{2k^2}{r^5}\dot{r}^2 + \frac{5gk}{7r^2} - \frac{\ell^2}{\hat{m}^2r^3} = 0. \tag{12}$$

By contrast, in the planetary problem, the radial equation takes the form of

$$\ddot{r} + \frac{GM}{r^2} - \frac{\ell^2}{m^2r^3} = 0. \tag{13}$$

Comparing Eqs. (12) and (13) we see that the funnel problem introduces two additional terms, one of which is proportional to $\dot{r}^2$, and so we would expect some deviation from the elliptical orbits of planets. These terms originate from the $\dot{z}^2$ kinetic energy term in Eq. (1) upon substitution of $z(r)$. Physically, the difference is that noncircular motion on the funnel always involves not just motion in the r and ϕ directions but also motion in the vertical (z) direction.

In fact, the only case where the results will carry over from the planetary problem is a circular orbit where $\dot{r}$ and $\ddot{r}$ are zero. Conversely, by inspection of Eq. (8) it follows that only this surface generates the required term proportional to r^{-2}. Hence, there is no surface that will generate all the Kepler orbits. We note that due to the appearance of the term containing $\dot{r}^2$ one can no longer define an effective potential as is standard for Eq. (13).

Note that Eq. (12) can also be written in terms of dimensionless variables as

$$\left(1 + \frac{\tilde{k}^2}{\tilde{r}^4}\right)\frac{d^2\tilde{r}}{d\tau^2} - \frac{2\tilde{k}^2}{\tilde{r}^5}\left(\frac{d\tilde{r}}{d\tau}\right)^2 + \frac{\tilde{k}}{\tilde{r}^2} - \frac{1}{\tilde{r}^3} = 0, \tag{14}$$

where $\tilde{k} = a^2k$. In order to plot the trajectories of the marble, we obtain an equation in which $\tilde{r}$ depends explicitly on ϕ by applying the transformation $u = 1/\tilde{r}$ and using the identity[6]

$$\frac{d\phi}{d\tau}\frac{d}{d\phi} = \frac{d}{d\tau}. \tag{15}$$

When working with dimensionless variables, these transformations lead to the expressions

$$\frac{d\tilde{r}}{d\tau} = -\frac{du}{d\phi}, \quad \frac{d^2\tilde{r}}{d\tau} = -u^2\frac{d^2u}{d\phi^2} \tag{16}$$

and so Eq. (14) can be rewritten as

$$-(1 + \tilde{k}^2u^4)\frac{d^2u}{d\phi^2} - 2\tilde{k}^2u^3\left(\frac{du}{d\phi}\right)^2 + 1 - u = 0. \tag{17}$$

Equation (17) cannot be solved analytically. Nevertheless, we can generate numerical solutions starting from particular initial conditions, $u(0)$ and $(du/d\phi)(0)$. All of our numerical solutions were obtained using MATHEMATICA 8.0, and the phase portrait diagrams were made using a freely available add-on package.[7]

First note that circular orbits occur only if $d\tilde{r}/d\tau = 0$. Using Eq. (11), this implies that for a circle of radius $\tilde{r} = R$, $d\tilde{z}/d\tilde{r} = 1/R^3$, i.e., that $R = 1/\tilde{k}$. For concreteness, let us now set $\tilde{k} = 1$. We then get one allowed circular orbit of radius $R = 1$. In ordinary (dimensional) units, this translates to $r = 7\ell^2/(5\hat{m}^2 g)$, according to Eq. (9) and the definition of $\tilde{k}$. As we would expect, the radius depends on the square of the angular momentum ℓ of the marble, and for a given angular momentum, only one radius is allowed.

What happens when $\tilde{r} \neq R = 1$? Figure 1 shows a numerical solution of Eq. (17); the polar plot shows the actual orbital shape that a marble would trace out on the funnel surface as seen from directly above the funnel. What is interesting is that unlike in the planetary problem, the orbits are generally not closed. The distance still oscillates between two radii, sometimes referred to as apsidal radii.[8] However, the phase $\phi(t)$ does not typically advance by 2π during one period of oscillation of the radius $\tilde{r}(t)$. More generally, if $\Delta\phi/(2\pi)$ is not a rational number, the orbit never closes. Since, by Eq. (3),

$$\Delta\phi = \int_0^T \frac{l}{\hat{m}\tilde{r}^2(t)}dt, \tag{18}$$

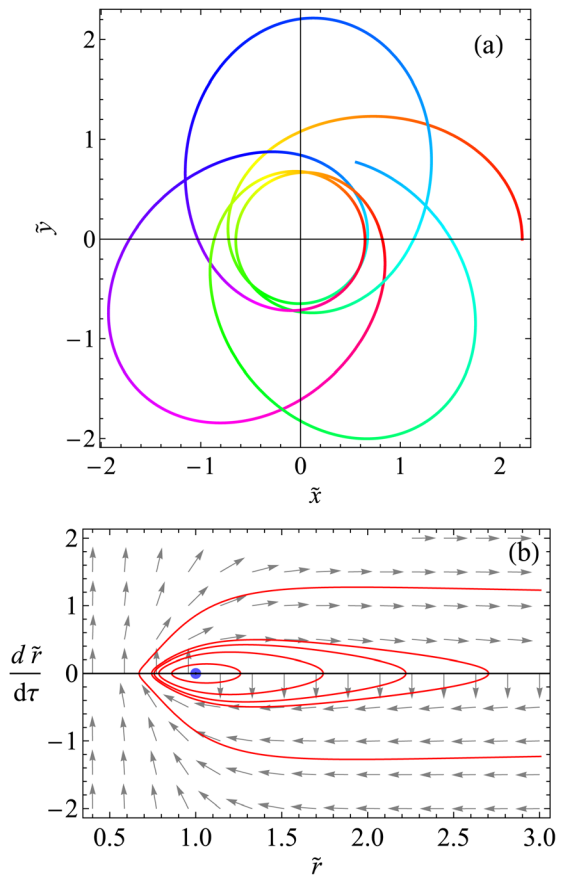

Fig. 1. The hyperbolic funnel: (a) One particular marble trajectory, with $\tilde{r}(0) = 2.22$ and $(d\tilde{r}/d\phi)(0) = 0$. (b) Phase space plot of the stability of the circular orbit. Note that the loops around the fixed point (circular orbit) represent solutions where $\tilde{r}$ oscillates between two extrema.

we see that only for very special initial conditions (a set of measure zero) can we expect closed orbits to arise, while the generic orbit will not be closed. Qualitatively, what we get instead is a "precession" of the orbital axis—a result that comes as no surprise to anyone who has ever closely observed a coin or marble rolling in a funnel.

To determine the stability of the orbits illustrated above, we now analyze the behavior of the solutions of the nonlinear system associated with Eq. (14) near equilibrium points. First, we rewrite Eq. (14) as a system,

$$\frac{d\tilde{r}}{d\tau} = v, \quad \frac{dv}{d\tau} = \frac{2v^2/\tilde{r}^5 + 1/\tilde{r}^3 - 1/\tilde{r}^2}{1/\tilde{r}^4}. \tag{19}$$

Its only equilibrium point, also called fixed point, is $(\tilde{r}, v) = (1, 0)$. Upon linearizing the system of Eq. (19) about $(1, 0)$ we obtain the Jacobian matrix

$$\begin{pmatrix} 0 & 1 \\ -\frac{1}{2} & 0 \end{pmatrix}, \tag{20}$$

whose eigenvalues are $\pm i\sqrt{2}/2$, and whose determinant and trace are 1/2 and 0, respectively. Hence, we can conclude that the equilibrium point (1, 0) is a center.[9,10] The phase plane plot shown in Fig. 1(b) depicts the fixed point (representing the circular orbit) as a dot on the horizontal axis; the solid lines depict the trajectories for a few other initial conditions. The plot clearly indicates that nearby trajectories around the fixed point are closed loops which are neither attracted nor repelled; thus, the circular orbit can be considered neutrally stable.[9] The loops enclosing the fixed point cross the horizontal axis at two points, and these two crossings define the smallest and largest distance of the marble from the funnel center. Again, the marble is seen to oscillate between these two apsidal radii.

IV. A SURFACE PROPORTIONAL TO r^{-2}

In this section, we consider a surface whose equation is given by $\tilde{z}(\tilde{r}) = -1/(2\tilde{r}^2)$. When we substitute this expression for $\tilde{z}$ into Eq. (11) several terms drop out, and we obtain

$$\left(1 + \frac{1}{\tilde{r}^6}\right)\frac{d^2\tilde{r}}{d\tau^2} - \frac{3}{\tilde{r}^7}\left(\frac{d\tilde{r}}{d\tau}\right)^2 = 0. \tag{21}$$

Interestingly, Eq. (21) can be analytically solved. We first reduce it to a first-order ordinary differential equation via the substitution

$$w(\tilde{r}) = \left(\frac{d\tilde{r}}{d\tau}\right)^2. \tag{22}$$

Since we now have two expressions for $dw/d\tau$,

$$\frac{dw}{d\tau} = \frac{dw}{d\tilde{r}}\frac{d\tilde{r}}{d\tau}, \qquad \frac{dw}{d\tau} = 2\frac{d\tilde{r}}{d\tau}\frac{d^2\tilde{r}}{d\tau^2}, \tag{23}$$

it follows that

$$\frac{d^2\tilde{r}}{d\tau^2} = \frac{1}{2}\frac{dw}{d\tilde{r}}. \tag{24}$$

Thus, Eq. (21) transforms into

$$\frac{1}{2}\left(1+\frac{1}{\tilde{r}^6}\right)\frac{dw}{d\tilde{r}}-\frac{3}{\tilde{r}^7}w=0. \tag{25}$$

We can easily solve Eq. (25) using calculus. First, we see that

$$\frac{dw}{d\tilde{r}}=\frac{3/\tilde{r}^7}{\frac{1}{2}(1+1/\tilde{r}^6)}\,w. \tag{26}$$

Therefore,

$$\frac{dw}{w}=\frac{6/\tilde{r}^7}{1+1/\tilde{r}^6}\,d\tilde{r}. \tag{27}$$

Now, integrating both sides yields

$$\ln w=-\ln\left(1+\frac{1}{\tilde{r}^6}\right)+\text{constant}. \tag{28}$$

Finally, after exponentiating both sides of Eq. (28), we obtain

$$w(\tilde{r})=\left(\frac{d\tilde{r}}{d\tau}\right)^2=\frac{c}{1+1/\tilde{r}^6}. \tag{29}$$

Here, we note that the constant c in Eq. (29) depends on the initial conditions for both $\tilde{r}(\tau)$ and $(d\tilde{r}/d\tau)(\tau)$. We also observe that an explicit solution to Eq. (29) expressed in terms of elliptic functions can be found for $\tilde{r}(\tau)$, and these solutions are plotted in Fig. 2. What is interesting about this family of solutions is that $\tilde{r}(\tau)$ does not oscillate in time for this surface; instead, it either monotonically increases towards infinity or decreases to zero. Normally, a spiraling motion into the funnel center can be attributed to energy loss. For this surface, however, the spiraling is a generic feature even in the absence of any energy dissipation, and we have in fact verified numerically that the total energy of the marble is conserved for all times for the kinds of motion shown in the figure. A similar behavior in this respect is exhibited by a point particle orbiting a center of attraction with a $1/r^3$ force law. Note, however, that in contrast to the central-force problem, in the funnel $\dot{r}$ goes to zero for small r (see Fig. 2).

To further investigate this type of motion, let us now examine actual marble trajectories. Figure 3(a) shows the polar plot of $\tilde{r}(\phi)$ for a particular set of initial conditions where $d\tilde{r}/d\phi$ is slightly negative. We again see that the radius of the orbit,

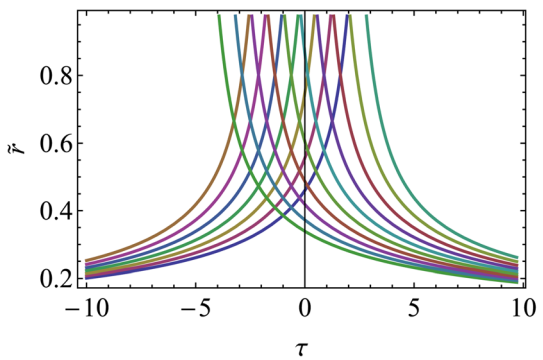

Fig. 2. Graph of exact solutions for $\tilde{r}(\tau)$ (elliptic functions), for an inverse-square funnel shape. Note that $\tilde{r}(\tau)$ monotonically tends to either zero or infinity, depending on the initial conditions.

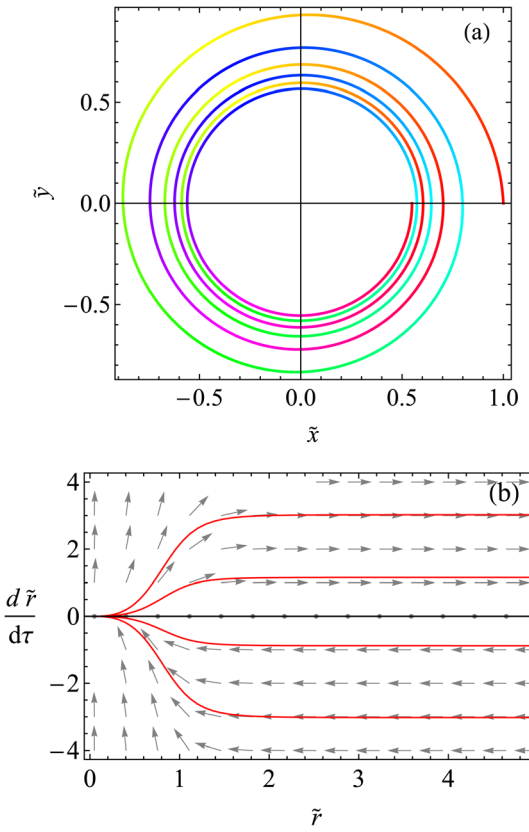

Fig. 3. Inverse-square funnel shape: (a) One particular marble trajectory for the initial condition of $\tilde{r}(0)=1$ and $(d\tilde{r}/d\phi)(0)=-0.05$. (b) The phase plane reveals that for $d\tilde{r}/d\tau>0$, $\tilde{r}$ increases with time towards infinity, and for $d\tilde{r}/d\tau<0$, $\tilde{r}$ decreases towards zero. None of the circular orbits (along the r axis) are stable against perturbations.

$\tilde{r}$, decreases steadily as the phase, ϕ, advances. This means that the marble gets sucked into the funnel over time. Its decrease in potential energy is compensated by an increase in the kinetic energy of revolution around the funnel center.

By means of a calculation similar to that for the hyperbolic surface, we find that circular orbits of any radius are possible for this surface, as we have an expression independent of the radius R of the circle. Now, the nonlinear system associated with Eq. (21) exhibits infinitely many equilibrium points of the form $(\tilde{r},0)$, i.e., the entire horizontal axis. The Jacobian matrix

$$\begin{pmatrix}0&1\\0&0\end{pmatrix} \tag{30}$$

has 0 as a repeated eigenvalue, which explains the line of equilibria,[10] and both the determinant and trace of this matrix are zero. Here can we can conclude only that the solution curves generally do not approach the line of equilibria, as corroborated by the phase plot in Fig. 3(b).

V. A SURFACE PROPORTIONAL TO r^{-3}

Finally, we look at $\tilde{z}(\tilde{r})=-1/\tilde{r}^3$ as the prescribed surface. In this case, Eq. (11) transforms into

$$\left(1+\frac{9^2}{\tilde{r}^8}\right)\frac{d^2\tilde{r}}{d\tau^2}-\frac{36^2}{\tilde{r}^9}\left(\frac{d\tilde{r}}{d\tau}\right)^2+\frac{3}{\tilde{r}^4}-\frac{1}{\tilde{r}^3}=0. \tag{31}$$

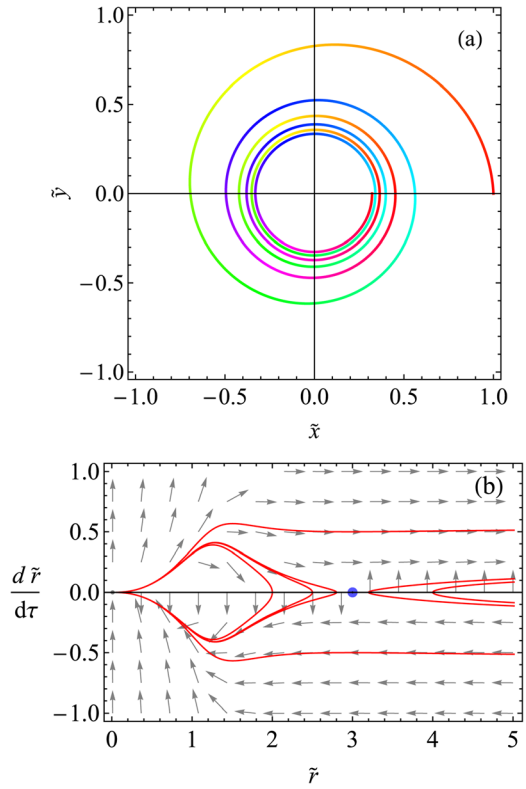

Fig. 4. (a) Trajectory on an r^{-3} surface, with the same initial conditions as in Fig. 3(a). (b) The phase-space portrait corresponding to this surface, revealing a saddle. In particular, follow the trajectories that approach the saddle point from either direction.

First, we observe that circular orbits of radius R occur when $R = 3$. For this particular surface, a new phenomenon appears near the equilibrium point (3, 0) for the associated nonlinear system. The Jacobian matrix is

$$\begin{pmatrix} 0 & 1 \\ 9/730 & 0 \end{pmatrix} \tag{32}$$

and has a negative determinant and a trace of zero. Two real distinct eigenvalues $\pm 3/\sqrt{730}$ occur, indicating that the fixed point (3, 0) is a saddle. Inspection of the phase portrait in Fig. 4(b) also reveals that along a line slanting up the saddle point is unstable (motion away from the fixed point), and along a perpendicular line sloping down it is stable (motion towards the fixed point). Overall, of course, a saddle means that the circular orbit is unstable for this surface, and we qualitatively recover some marble trajectories that are reminiscent from the r^{-2} surface. This is illustrated in Fig. 4(a), where the initial conditions are identical to those for the surface shown earlier in Fig. 3(a). Here, the approach into the funnel center proceeds somewhat more quickly. Interestingly, since the dynamics on this surface features a saddle point, it is possible to observe a trajectory where a spiral of increasing radius is followed by a spiral back to the funnel center, as illustrated in the phase space picture of Fig. 4(b). These trajectories arise when following the inner solid lines, which approach the fixed point at (3, 0). Such spirals reach a maximum (or minimum) radius before turning around, and they do not occur on the previous $(r^{-2}/2)$ surface.

Finally, we remark that a combination of the surfaces in Secs. III and V, i.e., $\tilde{z}(\tilde{r}) = -\tilde{r}^{-1} - \beta\tilde{r}^{-3}$, corresponds to the Schwarzschild potential around massive objects, such as black holes. In that case, we observe in the associated phase plot both a saddle and a center along the r axis. The center corresponds to bound orbits around the black hole, whereas the saddle connects to the origin. Interestingly, the dynamics near the origin reveals a major difference between the planetary (or central-force) problem and the funnel problem, in that for vanishing radii the radial speeds approach infinity in the former and zero in the latter.

VI. CONCLUSION

We have examined the motion of a small rolling marble on three different funnels, whose potentials are described by three different powers of r: –1, –2, and –3. For the first surface—the hyperbolic funnel—we found that the marble does not mimic planetary motion, except in the special case of circular orbits for which Kepler's third law holds. In general, however, the bound orbits traced out by the marble are not closed. For an inverse-square surface, an analytical solution for $r(t)$ can be obtained and we can show that all trajectories asymptotically approach either zero or infinity; here the circular orbits form a line of equilibria, but they are unstable against perturbations. For the inverse-cubic surface, the circular orbit is again unstable; however, the type of instability is different, as its associated fixed point is a saddle. This saddle allows for interesting trajectories characterized by the marble spiraling out from (or into) the center, turning around just before reaching the fixed point, and finally returning back to the funnel center (or to infinity). From a broader perspective, the intriguing result in this context is that fairly minor changes to the funnel surface shape can lead to qualitatively different orbital trajectories.

This problem, we believe, has pedagogical value in a junior/senior dynamics course. Since everyone has encountered coin funnels before, the problem will already be familiar to students, while also convincing them that certain systems are clearly more tractable in the Lagrangian formulation. Furthermore, this example showcases the power high-level mathematics software in finding and visualizing solutions to complicated nonlinear differential equations. Finally, the dynamical systems approach taken here may prove relevant in a course that also covers nonlinear dynamics: By applying the Lagrangian mechanics prescription in tandem with dynamical systems techniques, we arrive at a qualitative understanding of marble dynamics in funnels.

[1]G. D. White and M. Walker, "The Shape of the 'Spandex' and orbits upon its surface," Am. J. Phys. **70**, 48–52 (2002).
[2]L. A. Pars, *A Treatise on Analytical Mechanics* (Heinemann, London, 1965), chap. 8.
[3]L. D. Landau and E. M. Lifshitz, *Mechanics*, 3rd ed. (Butterworth-Heinemann, Burlington, MA, 1976), pp. 122–124.
[4]R. Talman, *Geometric Mechanics* (Wiley, New York, 2000), Chaps. 5 and 6.8.
[5]See, for instance, <http://www.funnelworks.com>.
[6]J. R. Taylor, *Classical Mechanics* (University Science Books, Sausalito, CA, 2005), Sec. 8.5.
[7]Wolfram Mathematica 8.0, with the add-on package "DiffEqs" available at <http://www.math.armstrong.edu/faculty/hollis/DiffEqs/>.
[8]H. Goldstein, C. P. Poole, and J. L. Safko, *Classical Mechanics*, 3rd ed. (Addison-Wesley, Reading, MA, 2001), chap. 3.
[9]S. H. Strogatz, *Nonlinear Dynamics and Chaos* (Addison-Wesley, Reading, MA, 1994), Chaps. 5.2 and 6.3.
[10]P. Blanchard, R. L. Davaney, and G. R. Hall, *Differential Equations* (Brooks/Cole, Pacific Grove, CA, 1998), p. 293 and p. 416.